PSFC/JA-07-15

Observation of Large Arrays of Plasma Filaments in Air Breakdown by 1.5 MW, 110 GHz Gyrotron Pulses

Hidaka, Yoshiteru; Choi, E.M.; Mastovsky, I.; Shapiro, M. A.;
Sirigiri, J. R.; and Temkin, R. J.

Plasma Science and Fusion Center
Massachusetts Institute of Technology
Cambridge MA 02139 USA

(Submitted to Physical Review Letters, October, 2007)

This work was supported by US AFOSR MURI04 program on the Nano-Physics of High Current Density Cathodes and Breakdown.

Observation of Large Arrays of Plasma Filaments in Air Breakdown by 1.5 MW, 110 GHz Gyrotron Pulses

Yoshiteru Hidaka, E. M. Choi, I. Mastovsky, M. A. Shapiro, J. R. Sirigiri, and R. J. Temkin

Plasma Science and Fusion Center, Massachusetts Institute of Technology, 167 Albany Street, Cambridge, Massachusetts 02139, USA

(Dated: October 5, 2007)

We report the observation of two-dimensional plasma filamentary arrays with more than one hundred elements generated during breakdown of air at atmospheric pressure by a focused Gaussian beam from a 1.5 MW, 110 GHz gyrotron operating in 3 microsecond pulses. Each element is a plasma filament elongated in the electric field direction and regularly spaced about one quarter wavelength apart in the plane perpendicular to the electric field. The development of the array is explained as a result of diffraction of the beam around the filaments, leading to the sequential generation of high intensity spots, at which new filaments are created, about a quarter wavelength upstream from each existing filament. Electromagnetic wave simulations corroborate this explanation and show very good correlation to the observed pattern of filaments.

PACS numbers: 52.80.Pi, 52.40.Db, 52.77.Fv, 52.38.Hb

We report the observation of large, two-dimensional regular arrays of plasma filaments generated during breakdown of air at atmospheric pressure by a focused Gaussian beam from a 1.5 MW, 110 GHz gyrotron with 3 μs pulse length. These filamentary arrays consist of a large number of regularly spaced elements, more than one hundred in some cases. They are observed both in volume breakdown and in breakdown at surfaces. The filamentary arrays are notably different from the well known filamentation observed in laser-induced plasmas. Laser generated filaments are aligned along the direction of propagation, while the filaments observed here are perpendicular to the direction of propagation. Each filament is aligned parallel to the direction of the electric field.

There is an extensive literature on gas breakdown at microwave frequencies [1–3] and at optical frequencies [4, 5]. Recent research has also addressed a number of important issues in breakdown at surfaces [6]. However, due to the scarcity of powerful sources in the millimeter wavelength range, there have been relatively few studies on gas breakdown at these wavelengths. Studies have been carried out with gyrotrons at frequencies of 35 to 86 GHz [7–10] at power levels up to 250 kW and pulse lengths of 0.05 to 20 ms. The available power in these studies was insufficient to achieve breakdown in air at atmospheric pressure, but careful studies were conducted either by using lower pressure (where the breakdown threshold is reduced), using alternate gases such as helium, or using initiators such as a collection of fine wires placed near the beam focus. These studies yielded some interesting evidence of filamentary structures in the breakdown volume. However, none of these studies produced the large, two-dimensional, filamentary regular arrays seen in the present experiments. Also, the present study differs substantially from these studies in terms of time scales (3 μs vs. 0.05-20 ms) as well as intensities (on the order of 10^6 vs. 10^4 W/cm^2) used for initiating and sustaining the breakdown plasma. A number of theoretical studies have also been reported to explain the structures such as "snakes" and "chains" that have been observed in high-pressure microwave breakdown research [11–13]. These explanations emphasize the role of plasma kinetics and instabilities. In this study, we explain the array as developing from a sequential process of electromagnetic wave diffraction. Incident microwave power is diffracted from plasma filaments formed early in the breakdown process.

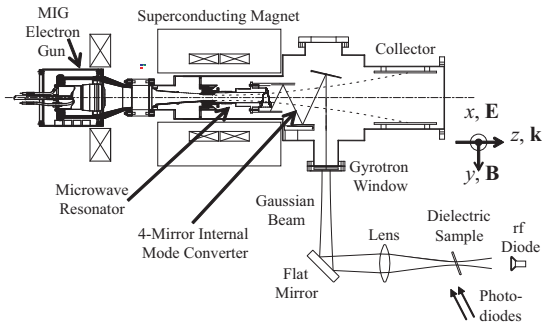

FIG. 1: Schematic of air breakdown experiments. Experiments were conducted with volume and (as shown) dielectric surface breakdown.

As the technology of high power millimeter wave sources matures and their applications broaden, breakdown will inevitably be an issue in transporting through a gas, or on the surface of a window through which such radiation is transmitted. This was our motivation for conducting volume and surface breakdown experiments in this relatively unexplored frequency band.

Figure 1 shows the experimental setup for the breakdown studies. The 110 GHz gyrotron, operating at 96

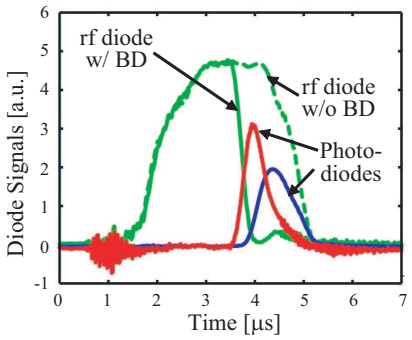

FIG. 2: Traces of rf diode and two photodiodes for a volume breakdown shot, and an rf diode trace when no breakdown occurs.

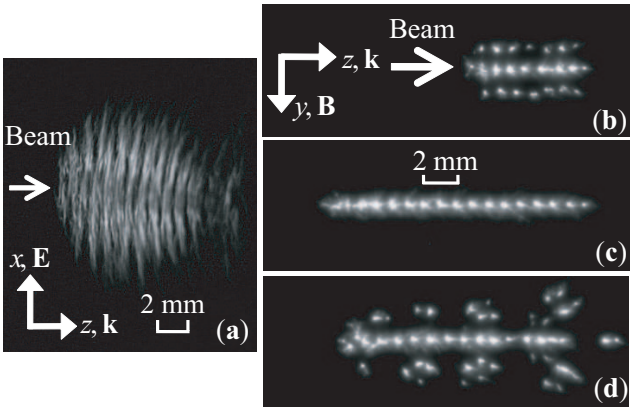

FIG. 3: Typical time-integrated volume breakdown plasma images in (a) E-plane and (b)-(d) H-plane. (camera exposure time >> pulse width)

kV beam voltage and 40 A beam current, can produce 1.5 MW of output power in 3 μs pulses [14]. The $TE_{22,6}$ mode generated in the resonator is then converted to a quasi-Gaussian output beam by a mode converter inside the gyrotron. The beam is linearly polarized in the x-axis as defined in Fig. 1, and has a waist at the output gyrotron window with a beam radius of 1.5 cm. This beam is further focused by a high density polyethylene (HDPE) lens with 14 cm focal length to a waist size of about 4 mm. For surface breakdown studies, a dielectric sample is placed at the beam waist, as shown in Fig. 1; it is absent for volume breakdown experiments. The tested dielectric materials included Lexan (polycarbonate), HDPE, and Teflon. No clear dependence on materials was found. An rf diode measures the transmitted beam power. Two fast photodiodes are positioned for studies of the breakdown delay time as well as the propagation direction and speed of the ionization front. An rf diode trace for a breakdown shot is shown in Fig. 2, along with the corresponding two photodiode signals and a transmitted power pulse without breakdown.

Figure 3 shows a typical volume breakdown for an incident 3 μs pulse with a field strength above 4.4 MV/m (2.5 MW/cm^2 in power density). Figure 3(a) shows the

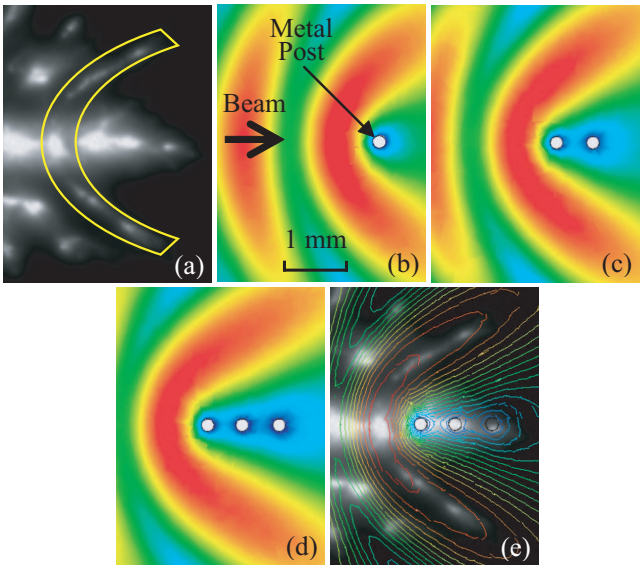

FIG. 4: (color online) (a) Volume breakdown image in H-plane with a crescent region enclosing a curved plasma structure of interest. E-field magnitude with (b) 1, (c) 2, and (d) 3 filaments modeled as metal posts (white circles) in simulations. (e) Superposition of (d) on top of (a).

time-integrated plasma image in the E-plane. The sensor of the digital camera was exposed during the entire pulse width. The observed plasma appears to consist of multiple filamentary plasma columns, instead of a single diffuse plasma. These filaments are parallel to the electric field. The filamentary array structure is more clearly confirmed in the H-plane (a plane perpendicular to the E-plane). Figures 3(b)-(d) show H-plane breakdown images from three different shots.

The remarkable feature of Figs. 3(b) - (d) is the observation of a regular, two-dimensional array of filaments. The filaments are found to have a typical radius of 0.1 to 0.2 mm, much smaller than the free space wavelength λ (= 2.73 mm) of the 110 GHz radiation. The average axial distance between adjacent filament centers on the beam axis is 0.76 mm with 10% standard deviation over many shots.

The same phenomenon as reported in this Letter was observed consistently in the experiments separated over many months with widely different experimental conditions such as air humidity as well as using a focusing lens made of Teflon with 18 cm focal length. Raising the field strength effectively up to 6 MV/m by using reflection from dielectric slabs also produced arrays of the same characteristics with slightly reduced regularity.

Figure 4(a) shows one of the typical filamentary array patterns seen in volume breakdown. The curved filamentary structure enclosed in the crescent region of Fig. 4(a) resembles the pattern of a wave diffracting around an obstacle. The obstacle would be the three rightmost filaments in this case. We believe that these patterns can be analyzed to show that diffraction plays an important

role in the development of the filamentary array.

From a series of measurements using the two axially displaced photodiodes, we have determined that breakdown is typically initiated in the focal region and propagates backwards towards the gyrotron power source. In Fig. 4(a), this would mean that breakdown first occurs at the point farthest to the right in the figure, and then develops backwards (to the left) with increasing time. Note that every experimental photograph presented in this Letter shows the entire emission history of an evolving array, and hence does not tell how large an emissive part of the array is at any one moment. For instance, in Fig. 2, the signal from the downstream photodiode (the earlier of the two photodiode signals) starts to decay even before the incident power starts to decay. This implies that the filaments generated downstream at an early stage extinguish before the end of the pulse. This is probably due to the microwaves being cut off or absorbed by new upstream filaments, and unable to sustain the old downstream filaments.

We observe experimentally that the initial breakdown produces a single filament that appears as a single breakdown spot in an H-plane view. We then use a theoretical model, based on the HFSS code [15] and, as shown in Figs. 4(b)-(d), to predict the subsequent development of the filamentary array. In the model, a Gaussian beam of $\sim$4 mm waist radius is excited in a box with radiation boundaries and a symmetry boundary. We assume that the initial filament develops a highly conductive plasma. The filament is thus modeled as a metal post, which is shown as a white circle in Fig. 4(b). This simulation shows that diffraction around the post results in a maximum field occurring approximately a quarter wavelength (= 0.68 mm) upstream of the metal post. Then, the next breakdown should occur near this maximum position. Assuming that breakdown does occur at that location, a second metal post will develop, as shown in Fig. 4(c). Diffraction will again result in a maximum field position roughly $\lambda/4$ upstream of the second metal post. Similarly, at the next stage, a third metal post is included in the simulation as shown in Fig. 4(d). From Fig. 4(d), we also see that diffraction will result in arcs of high intensity upstream from the three metal posts. The presence of filaments along such arcs is observed experimentally and can be clearly seen in Fig. 3(d) and Fig. 4(a). Figure 4(e) shows Fig. 4(a) with Fig. 4(d) overlaid on top. The curved structure falls well within the enhanced field region. Hence, we believe the enhanced field effect due to scattering plays a major role in determining where new filaments are created. In addition, the measured average axial filament distance of a quarter wavelength strongly corroborates this hypothesis. This distance also makes sense, considering that a field maximum is generated at a distance $\lambda/4$ upstream from a flat metal surface when a plane wave is reflected from that surface.

Filamentary arrays are also found to occur in surface breakdown. Surface breakdown has been studied by placing dielectric slabs at the beam waist formed by the focusing lens. Figure 5 shows a typical H-plane breakdown image with the beam incident on a tilted Lexan slab. The purpose of tilting is to minimize the reflected power propagating back to the gyrotron. Similar results were obtained for a range of different tilt angles. The photograph of Fig. 5 clearly demonstrates a highly periodic array of plasma filaments. There are usually two distinct breakdown regions with any tilt angle. In the region very close to the surface, the filaments (white circles in the H-plane) are arranged in layers parallel to the surface. In the region far from the surface, the filaments are aligned with the beam axis, as clearly seen in Fig. 5. In between these regions, the filaments show a transition from one alignment to the other and there may be dark spots, that is, filaments missing from the array.

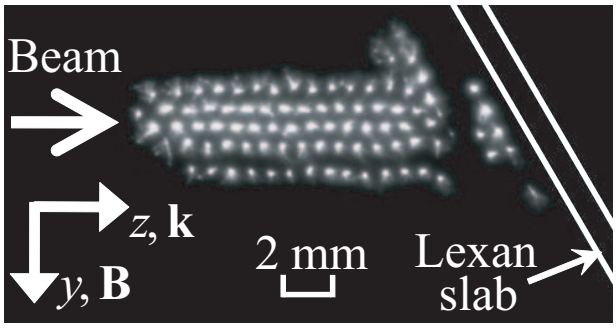

FIG. 5: Typical time-integrated surface breakdown plasma image in H-plane with a beam impinging on a dielectric surface. (camera exposure time >> pulse width)

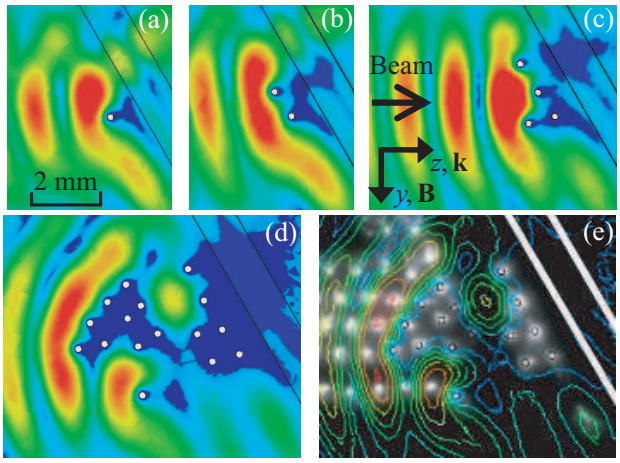

FIG. 6: (color online) Simulations of a filament propagation scenario in a surface breakdown, showing E-field magnitude when (a) 1, (b) 2, (c) 4, and (d) 16 filaments exist. (e) Expansion of Fig. 5 with (d) overlaid on top. Scale of (a) also applies to (b)-(e).

In the far region, the average axial distance (along the beam axis) between adjacent filament centers is determined to be 0.74 ± 0.06 mm, which is slightly larger than $\lambda/4$, as we have also observed in volume breakdown. Furthermore, this distance has no dependence on the tilt an-

gle of the slab. Thus, it appears that the presence of a dielectric surface has little effect on the mechanisms leading to the filamentary array aligned along the beam axis in the region far from the surface.

To explain the pattern near the surface in Fig. 5, we have carried out a series of simulations of the surface breakdown as shown in Fig. 6. In this model, a Lexan slab of 1.1 mm thickness is placed at the beam waist and tilted from the plane perpendicular to the beam by 30 degrees. Figure 6(a) assumes that one filament has already developed at the maximum field position created by reflection from the slab. As in the case of volume breakdown, the adjacent filament lies within the strongest field contour. Then, in Fig. 6(b), this new filament is modeled as another post. The resultant field distribution again fits with the locations of other nearby filaments. Figure 6(c) shows a possible next stage, after the appearance of two new posts (or filaments). Note that, as well as the most strongly enhanced region right near the existing filaments, there are always other enhanced field regions far from the dielectric surface, each of which is roughly a half wavelength apart. Since these regions are not as strong as the near-surface region, development of filaments in the far region requires more time. Eventually, however, a filament appears in the far region and often leaves a dark gap between the near-surface breakdown region and the far breakdown region as evident in Fig. 5. From this point on, the presence of the surface has little effect on the total field distribution, which is supported by the experimental fact that any tilt angle resulted in the same type of filamentary array with roughly identical spacing. A hypothetical later stage of the breakdown propagation with 16 existing filaments is simulated and shown in Fig. 6(d), and with the overlaid plasma image in Fig. 6(e). The contours show excellent agreement with the subsequent filament positions.

The model in Figs. 4 and 6 was based on an array of perfectly conducting metal posts, but a plasma filament will have a finite conductivity. The simulations have been repeated for posts with a range of conductivity values. We find that if the conductivity is less than $\sim$100 S/m, the reflected power is too weak to cause the large field enhancement seen in Figs. 4 and 6. A conductivity of 100 S/m or higher is expected if the plasma has an electron density n_e of 10^{16} cm^{-3} with an electron temperature T_e of 0.1 to 1 eV. These values for n_e and T_e have not been verified in the present experiments but are thought to be reasonable. The reflectivity of the filaments was also directly verified in the experiments. An rf diode detector was placed so as to measure power reflected from the breakdown region. A substantial amount of reflected power was detected whenever a breakdown occurred. Therefore, the filaments must have sufficient conductivity to be reflecting.

In summary, we have observed highly periodic, large, two-dimensional arrays of filamentary plasmas in atmospheric air breakdown with a MW-class, 110 GHz, linearly polarized Gaussian beam. The structured plasmas appear both in volume breakdown and surface breakdown. The most likely cause of the development of such a structure is sequential development of filaments by field enhancement approximately a quarter wavelength upstream of each existing filament. We have shown that the total field distribution due to scattering from filaments modeled as metal posts in the HFSS simulations corroborates well with the hypothesis above. The observed filamentary arrays look like photonic crystal structures. They may prove useful in guiding or manipulating beams of millimeter wave radiation.

This research was supported by the US AFOSR MURI04 program on the Nano-Physics of High Current Density Cathodes and Breakdown. The authors thank C. D. Joye for his help in imaging, and A. Neuber, G. Nusinovich and P. Woskov for helpful discussions.

REFERENCES

[1] A. D. MacDonald, *Microwave Breakdown in Gases* (Wiley, New York, 1966).
[2] Y. P. Raizer, *Gas Discharge Physics* (Springer, Berlin, 1991).
[3] A. V. Gurevich, N. D. Borisov, and G. M. Milikh, *Physics of Microwave Discharges* (Gordon and Breach, Amsterdam, 1997).
[4] N. Kroll and K. M. Watson, Phys. Rev. A **5**, 1883 (1972).
[5] Y. P. Raizer, *Laser-induced Discharge Phenomena* (Consultants Bureau, New York, 1977).
[6] A. Neuber, L. Laurent, Y. Y. Lau, and H. Krompholz, *Windows and RF Breakdown*, edited by R. J. Barker and E. Schamiloglu, High-Power Microwave Sources and Technologies, pp. 325-375 (IEEE Press, Piscataway, NJ, 2001).
[7] Yu. Ya. Brodskii *et al.*, Sov. Phys. JETP **57**, 989 (1983).
[8] A. L. Vikharev *et al.*, Sov. Phys. JETP **67**, 724 (1988).
[9] A. L. Vikharev *et al.*, Sov. J. Plasma Phys. **18**, 554 (1992).
[10] V. G. Brovkin and Yu. F. Kolesnichenko, J. Moscow Phys. Soc. **5**, 23 (1995).
[11] V. B. Gil'denburg and A. V. Kim, Sov. J. Plasma Phys. **6**, 496 (1980).
[12] O. A. Sinkevich and V. E. Sosnin, High Temperature **39**, 180 (2001).
[13] P. V. Vedenin and N. A. Popov, JETP **96**, 40 (2003).
[14] E. M. Choi *et al.*, Fusion Sci. Technol. **52**, 334 (2007).
[15] High Frequency Structure Simulator, www.hfss.com, Ansoft Corporation, Pittsburgh, PA, USA.